THE JOURNAL OF PHYSICAL CHEMISTRY C

Article

pubs.acs.org/JPCC

High-Conductance Conformers in Histograms of Single-Molecule Current−Voltage Characteristics

Wendu Ding, Christian F. A. Negre,* Leslie Vogt, and Victor S. Batista*

Department of Chemistry, Yale University, P.O. Box 208107, New Haven, Connecticut 06520-8107, United States

Energy Sciences Institute, Yale University, P.O. Box 27394, West Haven, Connecticut 06516-7394, United States

Supporting Information

ABSTRACT: Understanding charge transport across single molecular junctions is essential for the rational design and optimization of molecular device components. However, the correlation between calculated and experimental transport properties of single molecules probed by current−voltage (I−V) characteristics is often uncertain. Part of the challenge is that molecular conductance is sensitive to several factors that are difficult to control, including molecular orientation, conformation, aggregation, and chemical stability. Other challenges include the limitations of computational methodologies. Here, we implement the Σ-Extended Hückel (EH) nonequilibrium Green's function (NEGF) method to analyze the histogram of I−V curves of 4,4′-diaminostilbene probed by break-junction experiments. We elucidate the nature of the molecular conformations with a widespread distribution of I−V curves, typically probed under experimental conditions. We find maximum conductance for molecules that are not at the minimum energy configuration but rather are aligned almost parallel to the transport direction. The increased conductance is due to the more favorable electronic coupling between the transport channel state and the electronic states in the contacts, as indicated by the broadening of bands in the transmission function near the Fermi level. These findings provide valuable guidelines for the design of anchoring groups that stabilize conformations of molecular assemblies with optimal charge transport properties.

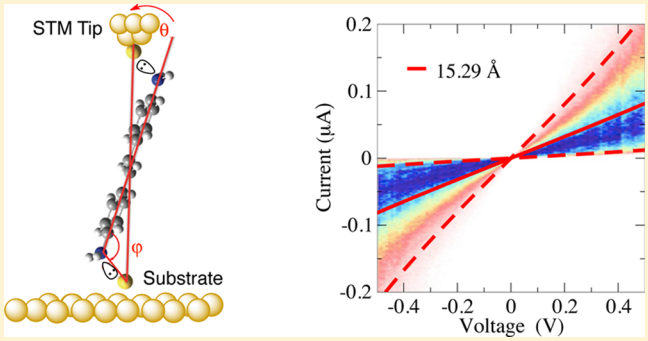

INTRODUCTION

Understanding single-molecule conductance is a subject of great technological interest and is central to the rational design and implementation of molecular electronic components.[1,2] Progress in the field, however, has been hindered by a significant gap between the theoretical predictions and experimental measurements as determined by various types of systematic uncertainties.[3] On the experimental front, one of the challenges has been to obtain reproducible data for the transport properties of *single* molecules bridging metallic contacts, since multiple contact junctions can usually be formed. In addition, significant uncertainty arises from structural and chemical instability, as well as from disorder due to a variety of possible molecular conformations and orientations. These challenges, in conjunction with the limitations of current computational methods, have made the comparison of experimental and calculated current−voltage (I−V) characteristic curves quite challenging. Calculations based on density functional theory (DFT), combined with nonequilibrium Green's function (NEGF) formulations, often predict conductance values that are at least an order of magnitude larger than the experimental data. DFT underestimates the molecular HOMO−LUMO energy gap,[3] giving a higher density of states (DOS) at the Fermi level and thus an overestimation of conductance. An approximate method has been proposed to improve DFT predictions by introducing self-energy corrections (DFT+Σ).[4−6] The method introduces a correction to HOMO and LUMO energy levels based on experimental values. However, methodologies that would ensure correlations between experimental and theoretical data without relying on empirical parameters have yet to be established.

Simulations of current−voltage (I−V) characteristics for molecular junctions in minimum energy configurations provide valuable insights but do not account for the widespread distribution of molecular conformations typically probed under experimental conditions.[3−5,7−10] Here, we focus on single molecule conductance curves of 4,4′-diaminostilbene (**1**) as characterized by scanning tunneling microscopy (STM) measurements of mechanically controllable break-junctions (Figure 1a).[9] In these experiments, the STM gold tip is brought in contact with the gold substrate in a solution of **1**. The tip is then withdrawn until the gold contact is broken and a single molecule bridges the gap between the tip and the

Received: March 31, 2014
Revised: April 4, 2014
Published: April 4, 2014

   dx.doi.org/10.1021/jp503193m | *J. Phys. Chem. C* 2014, 118, 8316−8321

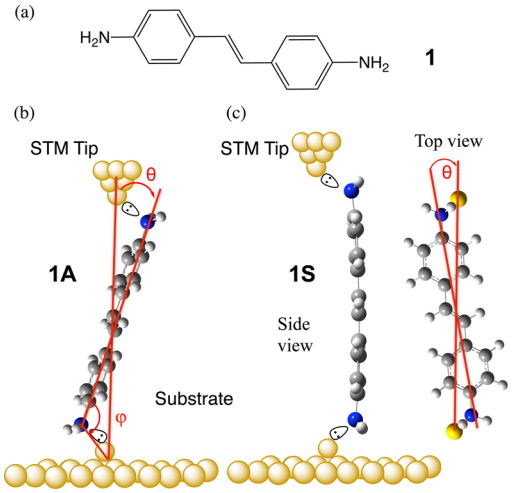

Figure 1. Conformers of 4,4′-diaminostilbene **1** (a), with gold atoms in *anti* (b) arrangement **1A** and *syn* position (side view (left) and top view (right)) **1S** (c) relative to the molecular plane. The improper dihedral angle, θ, defines the angle between the line connecting the two gold atoms and the axis connecting the two nitrogen atoms.

substrate (Figure 1b,c). The gap is then held for 150 ms while measuring the $I-V$ curve. Thousands of these measurements are then combined to build the complete histogram of characteristic curves determined by the resulting distribution of gaps and molecular conformations. The advantage of these measurements when compared to measurements on single junctions is that the resulting histograms are quite reproducible for a particular molecule−metal pair even when the individual metallic contacts and conformation of single molecules bridging the metallic gap might be difficult to reproduce. The outstanding challenge, however, is to understand the structural and conformational factors that characterize the spread of $I-V$ curves as resulting from the distribution of molecular orientations and the range of interlead distances probed by STM measurements.

Recent studies of $I-V$ histograms have been focused on the distribution of alignments and couplings,[11,12] the effect of the metal tip geometry on the width of the conductance histograms,[4,6,13] the junction evolution and reformation during these break-junction experiments,[5,13−15] and the distributions of defective junction structures as a function of temperature.[16] The effect of changing the nature of the anchoring groups has also been explored, including thiols that bind strongly and adopt multiple binding modes, cyanide groups that give low conductance, and pyridine and amine anchoring groups that exhibit small conductance fluctuations and reasonably high conductance.[13] However, the influence of molecular conformations on the transmission functions and on the distribution of $I-V$ curves has been thought to be negligible[4] and remains to be explored. Attempts to reproduce the current−voltage histogram have been recently made by Darancet et al. using the DFT+Σ method.[6] While this work showed improved results when compared to previous DFT calculations, only a small portion of experimental histograms was reproduced while the range of predicted curves did not cover the whole range of experimentally observed $I-V$ curves. Therefore, the interpretation of the experimental histograms through the assignment of configurations responsible for the observed dispersion of $I-V$ curves remains uncertain. Here, we focus on the effect of the position and orientations of the molecule relative to the gold contacts that have not been previously considered. We analyze junctions with various interlead distances within the range that allows for significant tunneling current. For each junction gap length, we analyze a Boltzmann distribution of molecular conformations characterized by DFT energies and $I-V$ curves computed with a practical approach based on the NEGF extended Hückel (EH) methodology (NEGF-EH) that provides accurate predictions of molecular conductance.[17] Our results indicate that the full range of $I-V$ curves can be assigned through the analysis of molecular conformers with significant conductance.

COMPUTATION METHOD

Structural models of **1** (Cartesian coordinates given in the SI) are prepared by DFT geometry optimization, using the B3LYP functional,[18] the 6-31++G(d,p) basis set[19] for C, N, and H, and the LANL2DZ basis set[20] for Au, as implemented in Gaussian 09.[21] The gold leads are represented by a single Au atom on each side of the molecule. The resulting global minimum energy geometry is the *anti* conformer **1A**, which binds through terminal amine groups connected to Au on either side of the molecular plane via lone pair interactions (Figure 1b). The *syn* conformer **1S** (Figure 1c) has the Au tips on the same side of the molecular plane and is only 0.12 kcal/mol less stable than **1A**. To explore the effect of molecular conformations on conductance, both **1A** and **1S** are reoptimized with the Au−Au distance constrained to be stretched or compressed by ±1.0 and ±2.0 Å. For each of these interlead distances, variations in θ (see Figure 1b,c) are also explored by constraining the Au−N−N angle (ϕ) during the DFT optimizations, resulting in 90 different positions and orientations of **1** relative to the Au contacts.

The transport properties of the molecular junctions generated by DFT geometry optimization were analyzed by using the NEGF-EH technique. The electron current flowing through **1** in contact with the Au electrodes is computed by integrating the transmission function $T(\varepsilon)$ according to the Landauer−Büttiker expression:[22,23]

$$I = \frac{2e}{h}\int_{-\infty}^{\infty} T(\varepsilon)[f_0(E-\mu_L) - f_0(E-\mu_R)]\,d\varepsilon \approx \frac{2e}{h}\int_{\mu_L}^{\mu_R} T(\varepsilon)\,d\varepsilon \quad (1)$$

where e is the electron charge, while $f_0(E-\mu_{L/R})$ is the room temperature Fermi−Dirac distribution with $\mu_{L/R}$ the Fermi energies of the left and right leads, respectively. The transmission function $T(\varepsilon)$ is defined according to the Fisher−Lee formula:[24] $T(\varepsilon) = Tr[\mathcal{G}_m(\varepsilon)\Gamma_L(\varepsilon)\mathcal{G}_m^{\dagger}(\varepsilon)\Gamma_R(\varepsilon)]$. Here, $\Gamma_{L/R}(\varepsilon) = i(\Sigma_{L/R}(\varepsilon) - \Sigma_{L/R}^{\dagger}(\varepsilon))$, with self-energies $\Sigma_L(\varepsilon) = V_L^{\dagger}\mathcal{G}_L(\varepsilon)V_L$ and $\Sigma_R(\varepsilon) = V_R\mathcal{G}_R(\varepsilon)V_R^{\dagger}$ defined in terms of the Green's functions of the isolated leads, $\mathcal{G}_{L/R}(\varepsilon) = (\varepsilon - H_{L/R})^{-1}$, and the electronic couplings $V_{L/R}$ defining the molecule-lead interactions.

The Au leads are modeled as single pseudoatoms with effective self-energies (Σ) that ensure a unit of quantum conductance for the transport properties of a reference Au-chain device, as implemented in the Σ-NEGF/EH methodology.[25−27] The resulting semiempirical approach gives semiquantitative agreement between calculated and experimental conductance data for a wide range of molecular frameworks (see the SI). Instead of correcting the levels of HOMO and

dx.doi.org/10.1021/jp503193m | J. Phys. Chem. C 2014, 118, 8316−8321

LUMO, as implemented in the DFT+Σ method,[4−6] the self-energies $\Sigma_{L/R}(\varepsilon) = \gamma^2 \mathcal{G}_{L/R}(\varepsilon)$ are defined by diagonal Green's functions $\mathcal{G}_{L/R}(\varepsilon) = -i/|\beta|$. The self-energies $\Sigma_{L/R}(\varepsilon) = -i\gamma^2/|\beta|$ are parametrized ($\Sigma_{L/R}(\varepsilon) = -2.0i$ for our calculations) to ensure the unit of quantum conductance (i.e., $G_0 = 2e^2/h = 7.75 \times 10^{-5}\ \Omega^{-1}$) for the reference device of a linear chain of Au atoms connected to the model leads at 0 V bias.[28,29]

An extended validation of the Σ-NEGF/EH methodology is presented in the SI, where we have analyzed three aspects of molecular conductance, including length dependence (see Figure S3, SI), dihedral angle dependence (see Figure S4, SI), and absolute molecular conductance (see Table S1, SI). We find that the methodology reproduces the length and angular dependence for a range of molecules, and predicts absolute experimental conductance values[30] with <30% error in most cases (similarly to the DFT+Σ method[6] albeit much more efficiently), while normal DFT overestimates conductance by at least 1 order of magnitude.[6]

RESULTS AND DISCUSSION

Figure 2 shows the comparison of the experimental histogram (a) and the calculated $I-V$ curves (b) colored according to the

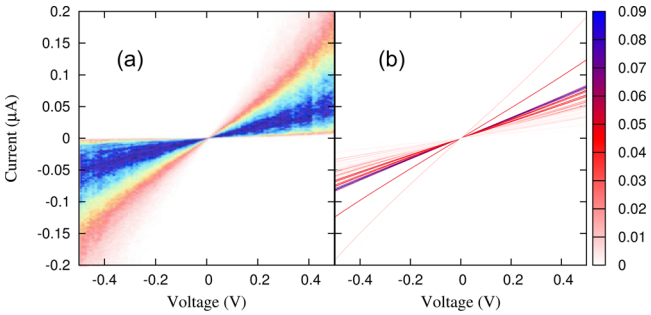

Figure 2. Comparison of the experimental histogram of $I-V$ curves (a)[30] and $I-V$ curves of 90 representative configurations for 4,4′-diaminostilbene, obtained by using the NEGF-EH method and colored according to the Boltzmann probability based on DFT energies (b).

Boltzmann probability. Figure 2 shows that the spread of calculated $I-V$ curves covers the entire range of $I-V$ characteristics observed in the experimental histogram, as determined by the transport properties for the single molecule junction for the various molecular orientations and interlead distances that give significant conductance, including configurations with transport properties that can easily differ from one another by as much as a factor of 4.

Figure 2 shows that comparisons between calculated and break-junction measurements cannot rely solely on the analysis of the minimum energy geometry of the system due to the distribution of configurations sampled by the experiments. In general, however, the minimum energy configuration has a characteristic with values of the same order of magnitude as the average experimental curve, although deviations of a factor 2−4 can be typically observed for a prototype system such as 4,4′-diaminostilbene. Consistently, the Σ-NEGF/EH method predicts a conductance of $(2.0 \times 10^{-3})G_0$, comparable to the experimental average value of $(1 \times 10^{-3})G_0$ and to the result obtained with the DFT+Σ method ($\approx(0.6 \times 10^{-3})G_0$).[6] These results represent a significant improvement compared to the previously reported NEGF-DFT method ($\approx(11 \times 10^{-3})G_0$).[6]

We emphasize, however, that the minimum energy configuration is responsible for one $I-V$ curve in the broad range of $I-V$ characteristics recorded in the experimental histogram, leaving a significant portion of the histogram unexplained, even when considering the different attachment modes that were previously analyzed.[6]

Figure 3 shows the $I-V$ curves of the optimized minimum energy configurations (solid lines), and configurations of maximum or minimum conductance (dashed lines), for various interlead distances superimposed to the experimental histograms.[9] These results include model junctions with fully optimized interlead configurations (central panels in Figure 3, parts a and b) and junctions with larger and smaller interlead distances as typically analyzed by studies of monatomic nanowires.[31] We find that the conductance of **1** is clearly reduced when the interlead separation is reduced from the optimized distance, with smaller currents originating from distorted molecular conformations. For gaps smaller than the optimized value, planar *anti* conformers do not fit well between the leads (see Figure 4). The resulting distortion misaligns the molecule relative to the transport direction and induces broken conjugation in the molecule itself. For larger interlead distances, the alignment between the molecule and the transport direction improves transport, but the overall conductance decreases due to the weaker molecule−lead electronic coupling determined by elongation of the N−Au distance. For *syn* conformers, stretching or shrinking the intertip distance also reduces molecular conductance since the molecule is bent into concave or convex configurations, altering its electronic structure.

The solid lines shown in Figure 3 overlay with the most likely $I-V$ curves probed by the break-junction measurements for the range of interlead distances that allow for significant current through **1**. However, it is necessary to consider a distribution of thermally accessible molecular orientations to account for the full range of measured conductance values. A key factor is the orientation of the molecule relative to the transport direction as determined by the improper dihedral angle (θ) between the two Au atoms and the longest molecular axis of **1** (Figure 1b,c). Dashed lines in Figure 3 show upper and lower bounds of the $I-V$ curves for conformers optimized with a set of fixed values of θ at a fixed interlead distance. We find that the conductance of **1A** shows a larger dependence on θ than **1S**. In the case of *anti* conformers, smaller θ corresponds to better alignment with the transport direction as well as shorter N−Au distance. Both of these geometrical factors increase conductance. For *syn* conformers, however, the optimized structure has almost optimal alignment with the transport direction (i.e., $\theta \approx 0$), so the characteristics obtained without constraining θ (solid lines in Figure 3) are very close to the upper bounds for this conformer. From the overlay of the models with experimental data, we conclude that the most likely junctions are formed by *syn* conformers, while the highest conductance measurements are the result of **1** binding in an *anti* configuration.

We note that most configurations yield lower conductance than the global minimum energy configuration. However, a few conformers of higher energy account for the largest conductance values. This is most evident for the case of **1A** at the optimum intertip distance (center panel in Figure 3a), for which the largest conductance is found only when the molecule is oriented to be more parallel to the transport direction (defined by the Au−Au vector). For a planar molecule, better alignment with the transport direction is achieved by increasing the angle Au−N−N (φ, in Figure 1) since the parallel

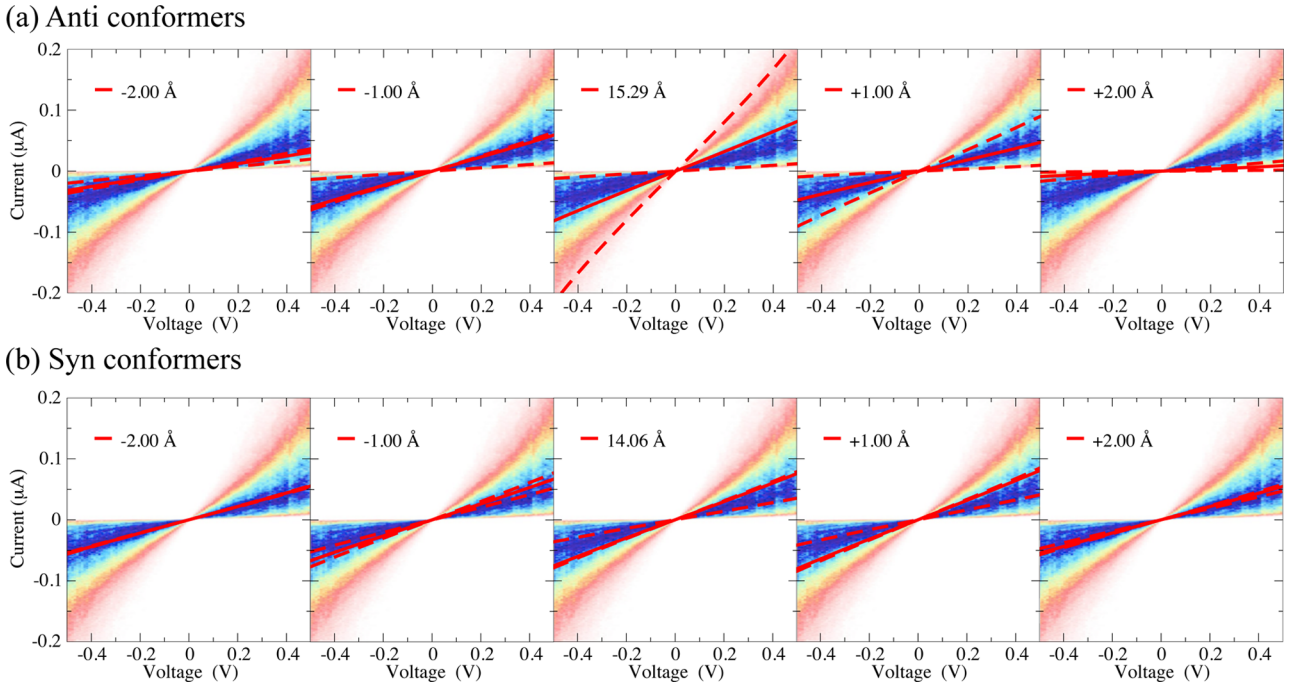

Figure 3. Calculated $I-V$ curves (red lines) for (a) **1A** and (b) **1S** in single-molecule junctions with varied intertip distances, superimposed on the experimental $I-V$ histogram shown in the background of each panel (measurement probability increases from red to blue) (adapted from ref 9). Results for the junction with an optimized intertip distance are shown in the center panels for both a and b. Plots to the left (right) of the center panel show $I-V$ curves for junctions with intertip distances decreased (increased) relative to the fully optimized configuration by ±1 and ±2 Å. In each panel, solid lines correspond to the optimized improper dihedral angle θ while the dashed lines show the upper and lower bounds for the range of possible $I-V$ curves as θ is varied.

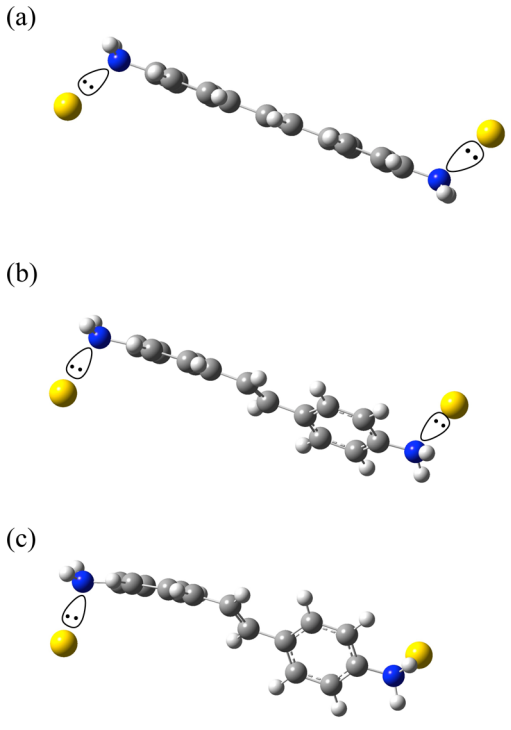

Figure 4. Optimized structures with varying Au–Au distances for **1A**. Minimum energy structures with Au–Au distance of (a) 15.3 (global minimum for **1A**), (b) 14.3, and (c) 13.3 Å.

alignment increases conductance. The angle φ changes with θ whenever the molecule remains attached to the leads. For the global minimum energy configuration, θ = 16.8°, giving φ = 117.5°. For the upper bound configuration of **1A** at the optimum interlead distance, however, θ = 14.6°, increasing φ to 124.6°, leading to a 1.5× increase in conductance at the Fermi level under 0 V bias.

To correlate the transport properties of **1A** with its orientation at the molecular junction, Figure 5 compares the transmission functions (TFs) for three selected conformers of **1A** at a contact junction with an interlead Au–Au distance of 15.3 Å, including the global minimum energy configuration, and the upper-bound and lower-bound conductance con-

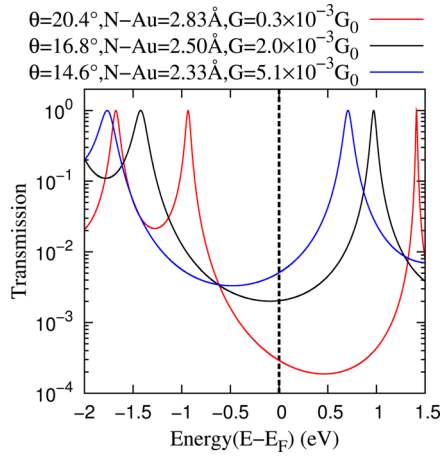

Figure 5. Transmission functions of three **1A** conformers with an interlead distance of 15.3 Å, including the global minimum energy conformer (black), the upper-bound conductance conformer (blue), and the lower-bound conductance conformer (red). The Fermi energy is defined by highest occupied gold orbitals. All three conformers have planar geometries.

dx.doi.org/10.1021/jp503193m | J. Phys. Chem. C 2014, 118, 8316–8321

formers. From the transmission functions, we observe that there are two effects when θ decreases and the molecule orients along the transport direction (Figure 5, curves red → black → blue). The first effect is that all molecular states are stabilized, as seen in the shift of TF peaks to lower energies. As a result, the tail of the TF peak corresponding to the molecular LUMO becomes closer to the Fermi level and increases the conductance relative to the fully optimized conformer. The second effect is the broadening of the peaks in the TF since the more aligned conformations have stronger couplings with the leads. This is clearly seen in the progression of widths from the low-conductance to the high-conductance conformers (see Figure 5). From Figure 5, we can observe that the broadening effect is more effective at increasing the overall area under the transmission function (within the integration window that determines the overall current) than the shifting of the energy levels. Although other authors attributed the increase in conductance to the shifting of HOMO (or LUMO) level toward the Fermi level,[32] we see that, in this case, the width of the transmission function is the dominant parameter.

Unfortunately, there is a limit to how much one can decrease θ at a given Au−Au separation before inducing molecular deformations. As the Au−N distance decreases, eventually there is not enough space for physisorbed binding between Au and N. In this case, constraining θ creates a similar effect as shrinking the intertip distance: the molecule twists and breaks the conjugation between the phenyl rings. For example, when φ is even 2.6° larger (i.e., more aligned to the transport direction) than in the upper-bound conductance conformer, the dihedral angle between the two phenyl rings increases to 55° (see Figure 6), breaking the conjugation and drastically reducing the

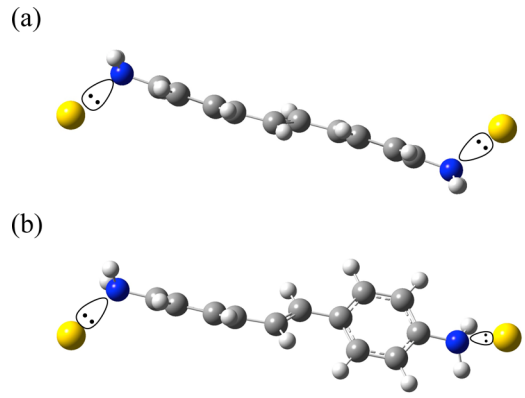

Figure 6. Optimized structure while constraining the Au−N−N angle ϕ for **1A** with a fixed intertip distance of 15.29 Å. (a) Structure with ϕ = 124.6°, which provides the global maximum conductance of $(5.1 \times 10^{-3})G_0$; (b) structure with ϕ = 127.2°, which provides a smaller conductance of $(2.0 \times 10^{-3})G_0$.

maximum molecular conductance of $(5.1 \times 10^{-3})G_0$ to an average conductance of $2(.0 \times 10^{-3})G_0$. This conformer is less likely to be seen experimentally observed, due to the internal strain and the resulting low conductance. In the case of larger interlead distances (e.g., 17.3 Å), θ = 8° can be obtained for planar molecules but the weaker coupling to the leads ultimately limits the conductance to low values due to the large Au−N distances.

In summary, it is clear that the range of calculated $I-V$ curves spans the entire histogram (Figure 3) when considering a range of conformers with varying values of θ for each interlead distance. Consistent with the experimental results,[30] we also observed that the probability of high-current conformers is quite low since such configurations are usually higher in energy than the minimum energy conformation. For example, the thermal probability of the conformer with the upper-bound $I-V$ curve at the optimized interlead distance for **1A** (see Figures 3 and 5) is only 0.6% relative to that of the global DFT minimum. This is consistent with low probability values found for the upper-bound edge of the experimental $I-V$ histogram.

Analogous observations on transport properties, as influenced by molecular conformation, can be made for **1** for which the geometry of the amine group makes high conductance conformers higher in energy than those with middle-range conductance. Upper-bound conformer has φ = 124.5°, which is much larger than a normal tetrahedral angle of 109.5°. The distortion raises the energy of the system and in turn lowers the probability of the conformer dramatically. These results complement earlier studies where the observed dispersion in the values of conductance was attributed only to the structure of the $NH_2-Au_{tip}/NH_2-Au_{substrate}$ link.[4] These findings clearly show that thermally accessible conformers that change the overall molecular orientation relative to the transport direction are necessary to account for the full range of observed molecular conductance. These observations suggest that optimization of the molecular orientation by molecular design might lead to aligned conformations with optimal transport properties.

■ CONCLUSIONS

We have found that amine linkers adopt a range of thermally accessible configurations in single molecule junctions, responsible for a distribution of experimental $I-V$ curves that can be properly described by the Σ-NEGF/EH methodology. The orientation of the molecule relative to the transport direction and the interlead distance are found to be the most significant geometrical parameters that determine the range of conductance values observed by experiments. Conformers with the highest conductance are typically aligned almost parallel to the transport direction and have optimal couplings with the metallic contacts. These findings are particularly valuable for the design of single-molecule junctions with optimal transport properties and reduced structural disorder.

■ ASSOCIATED CONTENT

Ⓢ Supporting Information

A detailed description and validation of the Σ-NEGF/EH methodology for calculations of $I-V$ characteristic curves and coordinates for the structural models reported in this paper. This material is available free of charge via the Internet at http://pubs.acs.org.

■ AUTHOR INFORMATION

Corresponding Authors

*E-mail: christian.negre@yale.edu.
*E-mail: victor.batista@yale.edu.

Notes

The authors declare no competing financial interest.

■ ACKNOWLEDGMENTS

We acknowledge high-performance computing time from NERSC and from the Yale University Faculty of Arts and Sciences High Performance Computing Center partially funded

by the National Science Foundation grant CNS 08-21132. The work on methods development was supported as part of the Argonne-Northwestern Solar Energy Research (ANSER) Center, an Energy Frontier Research Center funded by the U.S. Department of Energy, Office of Science, Office of Basic Energy Sciences under Award Number DE-SC0001059. We thank J. Widawsky and L. Venkataraman for providing the experimental histogram and for valuable comments.

REFERENCES

(1) Aviram, A.; Ratner, M. Molecular Rectifiers. *Chem. Phys. Lett.* **1974**, *29*, 277−283.
(2) Negre, C. F. A.; Gallay, P. A.; Sánchez, C. G. Model Non-Linear Nano-Electronic Device. *Chem. Phys. Lett.* **2008**, *460*, 220−224.
(3) Vélez, P.; Dassie, S. A.; Leiva, E. P. M. In *Recent Advances in Nanoscience*; Mariscal, M., Dassie, S. A., Eds.; Research Signpost: Trivandrum-Kerala, India, 2007; pp 1−38, .
(4) Quek, S. Y.; Venkataraman, L.; Choi, H. J.; Louie, S. G.; Hybertsen, M. S.; Neaton, J. B. Amine-Gold Linked Single-Molecule Circuits: Experiment and Theory. *Nano Lett.* **2007**, *7*, 3477−3482.
(5) Quek, S. Y.; Choi, H. J.; Louie, S. G.; Neaton, J. B. Length Dependence of Conductance in Aromatic Single-Molecule Junctions. *Nano Lett.* **2009**, *9*, 3949−3953.
(6) Darancet, P.; Widawsky, J. R.; Choi, H. J.; Venkataraman, L.; Neaton, J. B. Quantitative Current-Voltage Characteristics in Molecular Junctions from First Principles. *Nano Lett.* **2012**, *12*, 6250−6254.
(7) Muller, C. J.; van Ruitenbeek, J. M.; de Jongh, L. J. Conductance and Supercurrent Discontinuities in Atomic-Scale Metallic Constrictions of Variable Width. *Phys. Rev. Lett.* **1992**, *69*, 140−143.
(8) Quek, S. Y.; Kamenetska, M.; Steigerwald, M.; Choi, H. J.; Louie, S. G.; Hybertsen, M. S.; Neaton, J. B.; Venkataraman, L. Mechanically Controlled Binary Conductance Switching of a Single-Molecule Junction. *Nat. Nanotechnol.* **2009**, *4*, 230−234.
(9) Widawsky, J. R.; Kamenetska, M.; Klare, J.; Nuckolls, C.; Steigerwald, M. L.; Hybertsen, M. S.; Venkataraman, L. Measurement of Voltage-Dependent Electronic Transport across Amine-Linked Single-Molecular-Wire Junctions. *Nanotechnology* **2009**, *20*, 434009.
(10) Dell'Angela, M.; Kladnik, G.; Cossaro, A.; Verdini, A.; Kamenetska, M.; Tamblyn, I.; Quek, S. Y.; Neaton, J. B.; Cvetko, D.; Morgante, A.; Venkataraman, L. Relating Energy Level Alignment and Amine-Linked Single Molecule Junction Conductance. *Nano Lett.* **2010**, *10*, 2470−2474.
(11) Strange, M.; Thygesen, K. S. Towards Quantitative Accuracy in First-Principles Transport Calculations: The GW Method Applied to Alkane/Gold Junctions. *Beilstein J. Nanotechnol.* **2011**, *2*, 746−754.
(12) Williams, P. D.; Reuter, M. G. Level Alignments and Coupling Strengths in Conductance Histograms: The Information Content of a Single Channel Peak. *J. Phys. Chem. C* **2013**, *117*, 5937−5942.
(13) Hong, W.; Manrique, D. Z.; Moreno-García, P.; Gulcur, M.; Mishchenko, A.; Lambert, C. J.; Bryce, M. R.; Wandlowski, T. Single Molecular Conductance of Tolanes: Experimental and Theoretical Study on the Junction Evolution Dependent on the Anchoring Group. *J. Am. Chem. Soc.* **2012**, *134*, 2292−2304.
(14) Paulsson, M.; Krag, C.; Frederiksen, T.; Brandbyge, M. Conductance of Alkanedithiol Single-Molecule Junctions: A Molecular Dynamics Study. *Nano Lett.* **2009**, *9*, 117−121.
(15) Kim, T.; Darancet, P.; Widawsky, J. R.; Kotiuga, M.; Quek, S. Y.; Neaton, J. B.; Venkataraman, L. Determination of Energy Level Alignment and Coupling Strength in 4,4′-Bipyridine Single-Molecule Junctions. *Nano Lett.* **2014**, *14*, 794−798.
(16) Jones, D. R.; Troisi, A. Single Molecule Conductance of Linear Dithioalkanes in the Liquid Phase: Apparently Activated Transport Due to Conformational Flexibility. *J. Phys. Chem. C* **2007**, *111*, 14567−14572.
(17) Zahid, F.; Paulsson, M.; Polizzi, E.; Ghosh, W.; Siddiqui, L.; Datta, S. A Self-Consistent Transport Model for Molecular Conduction Based on Extended Hückel Theory with Full Three-Dimensional Electrostatics. *J. Chem. Phys.* **2005**, *123*, 064707.
(18) Lee, C.; Yang, W.; Parr, R. G. Development of the Colle-Salvetti Correlation-Energy Formula into a Functional of the Electron Density. *Phys. Rev. B* **1988**, *37*, 785−789.
(19) Hehre, W. J.; Radom, L.; Schleyer, P. v. R.; Pople, J. A. *Ab Initio Molecular Orbital Theory*; Wiley: New York, NY, 1986.
(20) Hay, P.; Wadt, W. R. Ab Initio Effective Core Potentials for Molecular Calculations - Potentials for K to Au Including the Outermost Core Orbitals. *J. Chem. Phys.* **1985**, *82*, 299−310.
(21) Frisch, M. J. et al. *Gaussian 09*, Revision A.1; Gaussian Inc.: Wallingford, CT, 2009.
(22) Landauer, R. Spatial Variation of Currents and Fields Due to Localized Scatterers in Metallic Conduction. *IBM J. Res. Dev.* **1957**, *1*, 223−231.
(23) Büttiker, M. Four-Terminal Phase-Coherent Conductance. *Phys. Rev. Lett.* **1986**, *57*, 1761−1764.
(24) Fisher, D. S.; Lee, P. A. Relation Between Conductivity and Transmission Matrix. *Phys. Rev. B* **1981**, *23*, 6851−6854.
(25) Paz, S. A.; Zoloff Michoff, M. E.; Negre, C. F. A.; Olmos-Asar, J. A.; Mariscal, M. M.; Sánchez, C. G.; Leiva, E. P. M. Configurational Behavior and Conductance of Alkanedithiol Molecular Wires from Accelerated Dynamics Simulations. *J. Chem. Theory Comput.* **2012**, *8*, 4539−4545.
(26) Negre, C. F. A.; Jara, G. E.; Vera, D. M.; Pierini, A. B.; Sánchez, C. G. Detailed Analysis of Water Structure in a Solvent Mediated Electron Tunneling Mechanism. *J. Phys.: Condens. Matter.* **2011**, *23*, 245305.
(27) Negre, C. F. A.; Milot, R. L.; Martini, L. A.; Ding, W.; Crabtree, R. H.; Schmuttenmaer, C. A.; Batista, V. S. Efficiency of Interfacial Electron Transfer from Zn-Porphyrin Dyes into TiO_2 Correlated to the Linker Single Molecule Conductance. *J. Phys. Chem. C* **2013**, *117*, 24462−24470.
(28) da Silva, E.; da Silva, A.; Fazzio, A. How Do Gold Nanowires Break? *Phys. Rev. Lett.* **2001**, *87*, 256102.
(29) Rubio-Bollinger, G.; Bahn, S.; Agraït, N.; Jacobsen, K.; Vieira, S. Mechanical Properties and Formation Mechanisms of a Wire of Single Gold Atoms. *Phys. Rev. Lett.* **2001**, *87*, 026101.
(30) Venkataraman, L.; Klare, J. E.; Nuckolls, C.; Hybertsen, M. S.; Steigerwald, M. L. Dependence of Single-Molecule Junction Conductance on Molecular Conformation. *Nature* **2006**, *442*, 904−907.
(31) Vélez, P.; Dassie, S.; Leiva, E. When Do Nanowires Break? A Model for the Theoretical Study of the Long-Term Stability of Monoatomic Nanowires. *Chem. Phys. Lett.* **2008**, *460*, 261−265.
(32) Kaliginedi, V.; Moreno-García, P.; Valkenier, H.; Hong, W.; García-Suárez, V. M.; Buiter, P.; Otten, J. L. H.; Hummelen, J. C.; Lambert, C. J.; Wandlowski, T. Correlations between Molecular Structure and Single-Junction Conductance: A Case Study with Oligo(phenylene-ethynylene)-Type Wires. *J. Am. Chem. Soc.* **2012**, *134*, 5262−5275.